Strength Growth as Chemo-Plastic Hardening in Early Age Concrete

By Franz-Josef Ulm[1] and Olivier Coussy[2]

ABSTRACT: This paper is concerned with modeling, identification, and experimental determination of thermo-chemo-mechanical couplings in early age concrete for the prediction of deformation and cracking on account of strength growth as chemo-plastic coupling within the theory of elastoplasticity. By applying the thermodynamic framework of reactive porous media to concrete at early ages, the coupling terms result from Maxwell symmetries. They lead to account for autogeneous shrinkage; hydration heat; and strength growth due to chemo-mechanical, thermo-chemical, and chemo-plastic coupling with a minimum of material parameters of clear physical significance and accessible by standard material tests. Furthermore, the diffusion of water through the layers of hydrates already formed is considered as the dominant mechanism governing the kinetics of hydration. To integrate this micromechanism in the macroscopic modeling, the "normalized affinity" is identified as an intrinsic kinetic function that characterizes the macroscopic hydration kinetics of concretes. Finally, by way of example, a Drucker-Prager criterion with isotropic chemical hardening is worked out that takes into account the evolution of the plastic properties (crack threshold and hardening/softening properties) with the hydration advancing.

INTRODUCTION

Concrete cracking at early ages is mainly caused by restrained thermal and chemical shrinkage, which induce a severe state of stress of a magnitude beyond the material strength developed. The thermal shrinkage occurs during cooling, and is thus related to the heat generation due to the exothermic nature of the hydration reaction, which, in the hours after pouring, may result in high temperature rises of up to 50°C in massive structures. The chemical shrinkage coupled with a capillary shrinkage is due to the consumption of water in the hydration reaction. It leads to an increasing pressure difference between the liquid and the gaseous phase (capillary pressure), balanced by compression of the concrete matrix, that induces a macroscopic shrinkage (see, for instance, Wittmann 1976; Buil 1979; Wittmann 1982; Acker 1988; Hua 1992; Baroghel-Bouny 1994). Furthermore, the creation of hydration products leads to stiffening of the matter, which—at the macrolevel of material description (i.e., scale of laboratory test specimen)—appears as a variation of the E-modulus in time. At a microlevel of material description, this aging cannot be regarded as an actual change of the elastic properties of the matter constituting concrete, but rather as a change in the concentration of the nonaging constituents (e.g., Bažant 1995), i.e., the hardened cement gel (roughly the tobermorite gel, consisting mainly of tricalcium and bicalcium silicate hydrates), and depends thus on the progress of the hydration reaction. In addition to this elastic aging, an evolution of the material strength with the creation of hydration products of concrete is observed (e.g., Mindess et al. 1978; Byfors 1980; Laube 1990), which influences the crack threshold and thus the cracking of concrete at early ages. These phenomenon are in competition: the greater the E-modulus, the greater are the stresses induced by restrained thermal and chemical shrinkage, which

might be of a magnitude beyond the material strength developed. The concrete then cracks, which affects the durability of the structure. This has prompted a surge of research activities since the mid-1980s in this domain, aiming at accurate modeling stresses in early age concrete, to prevent cracking (Acker 1988; Emborg 1989; Laube 1990; Bournazel 1992; Huckfeldt 1993; Laplante 1993; Tanabe and Ishikawa 1993; Torrenti et al. 1994; RILEM 1994; de Borst and van den Boogaard 1994).

This paper is concerned with modeling, identification, and experimental determination of thermo-chemo-mechanical couplings in early age concrete for the prediction of deformation and cracking at the macroscopic level of material description. It extends some recent works (Ulm and Coussy 1995) to the case of irreversible skeleton evolution (i.e., cracking) on account of chemo-plastic couplings to model strength growth as chemical hardening within the theory of elastoplasticity.

MACROSCOPIC MODELING OF HYDRATION REACTION

Hydration of cement is a fairly complex set of competing chemical reactions of different kinetics and amplitudes, related to complex physico-chemical phenomena at the microlevel of material description. For the modeling, the hydration may be roughly viewed as follows (Fig. 1): at instant t, the solid part of the matter is formed of unhydrated cement and hydrates. In order for the reaction to occur, water diffuses through the layers of hydrates already formed to the unhydrated cement. Once they meet, new hydrates are formed in an instantaneous manner relative to the time scale of the microdiffusion process; then the water is chemically or physically combined. Hence, the diffusion of water through the layers of hydrates may be considered as the dominant mechanism regulating the reaction kinetics.

To integrate this chemical reaction in the constitutive equations that aim at predicting macroscopic strains, stresses, and cracking, concrete will be considered as a porous medium composed of a skeleton and fluid phases. The observable strain is that of the skeleton and is noted ε. Moreover, cracking will be considered here within the standard continuum approach of elastoplasticity through some plastic variables, namely the plastic (or permanent) strain tensor ε^p, and the hardening/softening variable χ, which both model the irreversible skeleton evolutions associated with concrete cracking. Furthermore, for the sake of clarity, the medium is considered as closed with respect to the fluid phases saturating the porous space (i.e., no

[1]Res. Engr., Docteur-Ingénieur, Laboratoire Central des Ponts et Chaussées, Div. Bétons et Ciments pour Ouvrage d'Art, Section Comportement Mécanique et Modélisation, 58 Bd. Lefebvre, 75732 Paris Cedex 15, France.

[2]Dir. of Res., Docteur ès Sciences, Laboratoire Central des Ponts et Chaussées, Service Modélisation pour l'Ingénieur, 58 Bd. Lefebvre, 75732 Paris Cedex 15, France.
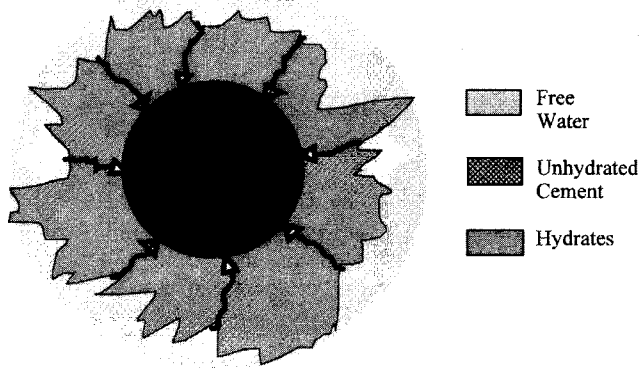
FIG. 1. Hydration Sketch: Microdiffusion of Free Water through Layers of Already Formed Hydrates to Unhydrated Cement

exchange with the exterior). With respect to the considered hydration sketch, only the liquid water phase is considered as active in the medium, and the mass conservation of the liquid phase reads

$$\frac{dm_l}{dt} = -\frac{dm_{l \to sk}}{dt} \qquad (1)$$

where m_l = variation in water mass per unit of macroscopic volume; and $m_{l \to sk}$ = the water mass per unit of volume that combines with cement to form hydrates, which is considered to become part of the skeleton (physically and/or chemically combined). Eq. (1) makes use of two simplifying hypotheses: (1) that the system is closed with respect to external flow (no external supply of water mass during hydration); and (2) that the water phase in the porous medium is only involved in the liquid-solid phase change of the hydration reaction. Independent of these hypotheses, $m_{l \to sk}$ = increase of skeleton mass per unit of volume.

For the constitutive modeling the thermodynamic framework of reactive porous media (Coussy 1995) is applied to concrete at early ages (Ulm and Coussy 1995) to account at the macrolevel of material description for the hydration reaction and its interaction with temperature evolution (thermochemical coupling), with skeleton strain (chemo-mechanical coupling), and with irreversible skeleton evolution (chemoplastic coupling). To this end, we recall the second law of thermodynamics that states that the internal entropy variation dS is greater than or equal to the entropy supplied from the exterior. In the case of a closed system this entropy supply from the exterior is only provided by heat exchange with the exterior $Q^0 \, dt$, thus around a reference temperature T_o

$$\frac{dS}{dt} \geq \frac{Q^0}{T_o} \qquad (2)$$

Furthermore, the difference between the left and right hand side of (2) is due to internal entropy production associated with dissipative phenomena. The entropy balance thus reads

$$T_o \frac{dS}{dt} = Q^0 + \varphi \qquad (3)$$

where φ = dissipation; and φ/T_o = internal entropy production rate due to dissipation. Considering concrete at early ages, this dissipation can primarily be attributed to irreversible skeleton evolutions and to the action of the hydration reaction. The latter reads formally

$$\varphi_{\to sk} = (g^l - G) \frac{dm_l}{dt} \geq 0 \qquad (4)$$

where g^l = free mass enthalpy (or chemical potential) of the

free water; and G = chemical potential of the water combined in the solid phase. The potential difference $g^l - G$ expresses thus the (thermodynamic) imbalance between the free water and the water combined in the solid phase, and is the driving force of the microdiffusion process governing the hydration reaction. The previous equation can be equally written in the form

$$\varphi_{\to sk} = A_m \frac{dm}{dt} \geq 0 \qquad (5)$$

where A_m = affinity, while the subscript on $m = m_{l \to sk}$ has been omitted. From the standpoint of standard thermodynamics, the previous expression of the hydration reaction dissipation, leads to identify formally affinity A_m as the thermodynamic force associated with the skeleton solidification rate $\dot{m} = dm_{l \to sk}/dt$. Now, recall the expression of the dissipation of the closed system, which includes the dissipation due to permanent skeleton evolution as well as the one associated with the hydration reaction [i.e., (4) or (5)]

$$\varphi = \sigma : \dot{\varepsilon} - S\dot{T} - \dot{\psi} \geq 0 \qquad (6)$$

where σ = macroscopic stress tensor; and ψ = the free energy of the closed system. The latter reads as a function of the external state variables, absolute temperature T, and strain tensor ε, and of the internal state variables, the plastic variables, ε^p and χ, associated with irreversible skeleton evolution and skeleton mass m involved in the hydration reaction, thus formally

$$\psi = \psi(T, \varepsilon, \varepsilon^p, \chi, m) \qquad (7)$$

Then, using (7) in (6), leads to

$$\varphi = \left(\sigma - \frac{\partial \psi}{\partial \varepsilon} \right) : \dot{\varepsilon} - \left(S + \frac{\partial \psi}{\partial T} \right) \dot{T} + \sigma : \dot{\varepsilon}^p + \zeta \dot{\chi} + A_m \dot{m} \geq 0 \qquad (8)$$

In the previous inequality, some well known results of standard thermodynamics of continuum mechanics have been combined with the explicit identification (5) of affinity A_m as the thermodynamic force associated with the solidification rate $\dot{m}$. In fact, the first four terms of inequality (8) are those of an ordinary elastoplastic solid, for which the state equations read (e.g., Lemaitre and Chaboche 1990; Coussy 1995)

$$\sigma = \frac{\partial \psi}{\partial \varepsilon} = -\frac{\partial \psi}{\partial \varepsilon^p}; \quad S = -\frac{\partial \psi}{\partial T}; \quad \zeta = -\frac{\partial \psi}{\partial \chi} \qquad (9a\text{–}c)$$

with ζ = hardening force, while the last term results from (5) and implies

$$A_m = -\frac{\partial \psi}{\partial m} \qquad (9d)$$

It states that the imbalance between the free water and the water combined in the solid phase derives in the case of a closed system from free energy ψ. Using these results, the thermo-chemo-mechanical couplings in the modeling result from the Maxwell symmetries applied to (9). More precisely, differentiating the preceding state equations leads to the incremental state equations

$$d\sigma = \frac{\partial^2 \psi}{\partial \varepsilon^2} : (d\varepsilon - d\varepsilon^p) + \frac{\partial^2 \psi}{\partial \varepsilon \partial T} dT + \frac{\partial^2 \psi}{\partial \varepsilon \partial m} dm \qquad (10)$$

$$dS = -\frac{\partial^2 \psi}{\partial T^2} dT - \frac{\partial^2 \psi}{\partial T \partial \varepsilon} : (d\varepsilon - d\varepsilon^p) - \frac{\partial^2 \psi}{\partial T \partial m} dm \qquad (11)$$

$$d\zeta = -\frac{\partial^2 \psi}{\partial \chi^2} d\chi - \frac{\partial^2 \psi}{\partial \chi \partial m} dm \qquad (12)$$

$$dA_m = -\frac{\partial^2 \psi}{\partial m \partial \varepsilon}:(d\varepsilon - d\varepsilon^p) - \frac{\partial^2 \psi}{\partial T \partial m} dT - \frac{\partial^2 \psi}{\partial \chi \partial m} d\chi - \frac{\partial^2 \psi}{\partial m^2} dm \tag{13}$$

In (10)–(13), the second order derivatives of free energy ψ respect the Maxwell symmetries, consequence of the chosen thermodynamic approach, and include the thermo-chemo-mechanical couplings of the modeling. Their physical significance will be successively derived in what follows.

Aging Elasticity, Thermal Dilatation, Capillary Shrinkage

Inverting state in (10) leads to

$$d\varepsilon = \mathbf{C}^{-1}:d\sigma + d\varepsilon^p + \mathbf{a}dT + \mathbf{b}dm \tag{14}$$

that allows for the following identifications:

- $\mathbf{C} = \partial^2 \psi / \partial \varepsilon^2 =$ (tangent) elastic stiffness tensor. In the case of early age concrete, these elastic properties increase with the hydration advancing, and depend thus on the solidification mass m [aging elasticity, i.e., $\mathbf{C} = \mathbf{C}(m)$], as also pursued by Bažant and co-authors (Bažant 1977; Bažant and Prasannan 1989a,b; Carol and Bažant 1993).

- $\mathbf{a} = -\mathbf{C}^{-1}:\partial^2 \psi / \partial \varepsilon \partial T$ is the tensor of (tangent) thermal dilatation coefficients, which due to thermo-mechanical coupling relates the temperature variation dT to the macroscopic unrestrained strain of thermal origin ($d\varepsilon^t = \mathbf{a}dT$). In turn, the second-order tensor $\mathbf{A} = \partial^2 \psi / \partial \varepsilon \partial T$ presents the stress per unit of temperature variation induced by restrained thermal swelling or shrinkage.

- $\mathbf{b} = -\mathbf{C}^{-1}:\partial^2 \psi / \partial \varepsilon \partial m$ is the tensor of (tangent) chemical dilatation coefficients (positive for unrestrained isothermal swelling and negative in the case of shrinkage), which relates the increase in solidification mass m to the strains of chemical origin ($d\varepsilon^c = \mathbf{b}dm$). It accounts for hydration shrinkage and related capillary shrinkage. The hydration shrinkage is caused by the volume change due to the hydration of cement (Le Chatelier consumption). The consumption of water by the hydration reaction [i.e., (1)] leads to the formation of menisci with an increasing pressure difference (capillary pressure) between the liquid (free water) and the gaseous phase saturating the porous space. Consequently, the skeleton suffers an increasing internal compression, inducing an overall (capillary) shrinkage, that depends on the quantity of water combined by hydration in the solid phase, and thus on solidification mass m. Consequently, tensor $\mathbf{B} = \partial^2 \psi / \partial \varepsilon \partial m$ presents the (tensile) stress per unit of solidification mass induced by restrained chemical/capillary shrinkage. Due to the physical origin of the capillary shrinkage, the relation which links the solidification mass and the strain is eventually nonlinear [i.e., $\mathbf{b} = \mathbf{b}(m)$].

Finally, in the isotropic case, for which $\mathbf{a} = \alpha\mathbf{1}$ and $\mathbf{b} = \beta(m)\mathbf{1}$, state (10) reads

$$d\sigma = \frac{E(m)}{1 + v} (de - de^p)$$

$$+ \frac{E(m)}{3(1 - 2v)} (d\varepsilon - d\varepsilon^p - 3\alpha dT - 3\beta dm)\mathbf{1} \tag{15}$$

where $\mathbf{1} =$ second order unit tensor. In the previous equation, $de = d\varepsilon - (1/3)d\varepsilon\mathbf{1}$ and $de^p = d\varepsilon^p - (1/3)d\varepsilon^p\mathbf{1}$ are the deviator parts of the total and the plastic strain increments, and $d\varepsilon = \text{tr}(d\varepsilon)$ and $d\varepsilon^p = \text{tr}(d\varepsilon^p)$ the corresponding incremental total and plastic volume variation. Furthermore, referring to experimental results, the aging elasticity is expressed by the de-
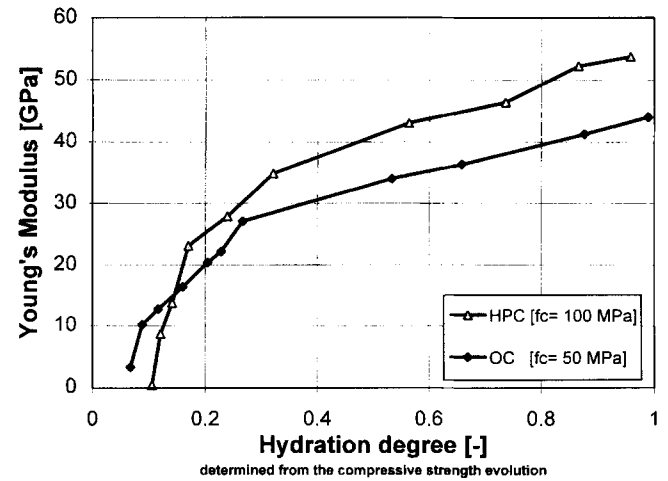

FIG. 2. Aging Elasticity: Evolution of Young's Modulus E as Function of Hydration Degree for High Performance Concrete [HPC, $E(\infty) = 54$ GPa] and Ordinary Concrete [OC, $E(\infty) = 44$ GPa] (Experimental Values from Laplante 1993)

pendence of the Young's modulus E on solidification mass m, as illustrated in Fig. 2, for a high performance concrete and an ordinary concrete. In return, Poisson ratio v can be assumed constant.

Exothermic Nature of Hydration Reaction

Using state equation (11) in (3), the thermal equation reads

$$C_\varepsilon \dot{T} - T_o\mathbf{A}:(\dot{\varepsilon} - \dot{\varepsilon}^p) - L_m\dot{m} = Q^0 + \varphi \tag{16}$$

where $Q^0 = r - \text{divq}$ presents the rate of external heat supply provided by conduction (term $-\text{divq}$, with $\mathbf{q} = -\vec{k}\mathbf{1} \cdot \text{grad}T$ the heat flux vector when adopting a linear isotropic conduction law) and by volumic heat sources (term r). The physical significance of the terms on the left-hand side of (16) have been discussed in some detail in Ulm and Coussy (1995), in particular

- $C_\varepsilon = T_o\partial^2 \psi / \partial T^2 =$ volume heat capacity per unit of volume (i.e., the heat required to produce a unit temperature variation).

- $T_o\mathbf{A} = T_o\partial^2 \psi / \partial T \partial \varepsilon$ is the latent heat per unit of (elastic) deformation $d\varepsilon - d\varepsilon^p$, and constitutes the counterpart of the thermo-mechanical coupling presented previously. It can be considered negligible with respect to the hydration heat generation.

- $L_m = T_o\partial^2 \psi / \partial T \partial m$ is the latent heat of the hydration reaction per unit of solidification mass dm, which is positive due to the exothermic nature of the hydration reaction and which is assumed constant. Note that the heat given out by the hydration reaction is due to latent heat effects ($L_m > 0$ due to the exothermic nature of the hydration reaction), as well as due to the hydration dissipation $\varphi_{\to sk}$ (positive due to the second law), even though the latter can be considered as negligible with respect to the exothermic latent hydration heat. The same reasoning can be applied to the dissipation associated with irreversible skeleton evolutions, as well as to the latent heat of (elastic) deformation. Then, heat equation (16) becomes

$$C_\varepsilon \dot{T} = Q^0 + L_m\dot{m} \tag{17}$$

which is the heat equation generally used.

Strength Growth As Chemical Hardening

For the modeling of early age concrete cracking, two phenomena need to be taken into account: on the one side the irreversible skeleton evolution, taken into account here within

the standard continuum approach of elastoplasticity through some plastic variables, the plastic (or permanent) strain tensor $\boldsymbol{\varepsilon}^p$, and the hardening/softening variable χ; and on the other side, the evolution of the crack threshold with the hydration advancing.

As in the standard plastic model, a loading point $\boldsymbol{\sigma}$ cannot lie outside of elasticity domain C_E of the material, which depends on the hardening/softening state through hardening force ζ. The plastic admissible stress states thus read in a standard manner

$$\boldsymbol{\sigma} \in C_E \Leftrightarrow f(\boldsymbol{\sigma}, \zeta) \leq 0 \qquad (18)$$

where $f(\boldsymbol{\sigma}, \zeta)$ = loading function. Evolutions of the plastic variables $\boldsymbol{\varepsilon}^p$ and χ only occur if a loading point is at the boundary of elasticity domain C_E and where it remains ($f = df = 0$). However, in contrast to the standard plastic model, where the evolution of the hardening force depends only on the plastic hardening/softening variable χ [i.e., $\zeta = \zeta(\chi)$], incremental state equation (12) accounts for a further dependence on the hydration mass m. This is the phenomenon of chemical hardening. Noting U the part of the free energy that is related to the hardening/softening phenomena, we have

$$d\zeta = -\frac{\partial^2 U}{\partial \chi^2} d\chi - \frac{\partial^2 U}{\partial \chi \partial m} dm \Leftrightarrow \zeta = -\frac{\partial U(\chi, m)}{\partial \chi} = \zeta(\chi, m) \qquad (19)$$

More precisely, the effect of chemical hardening is twofold: it concerns the initial material threshold at the onset of plastic evolutions for a given hydration state, i.e., the strength growth strictly speaking, as well as the plastic hardening/softening properties of the material when irreversible skeleton evolutions occur. Concerning the evolution of material strength, it has been shown experimentally that the compressive strength of concrete increases quasi linearly with the hydration products (e.g., Mindess et al. 1978), and thus with solidification mass m. Less has been reported on the hardening/softening behavior of concrete at early ages. In a first approach, a linear chemo-plastic coupling will be assumed by applying the following expression for hardening energy U:

$$U(\chi, m) = -\zeta_\infty m\chi + mU_\infty(\chi) \qquad (20)$$

which, using (19)

$$\zeta = m\zeta_\infty - m\frac{\partial U_\infty(\chi)}{\partial \chi} \qquad (21)$$

leads to a linear dependence of hardening force ζ on solidification mass m. This linear dependence concerns both the initial material threshold $m\zeta_\infty$ (strength growth), and its evolution due to plastic evolutions $-m\partial U_\infty/\partial \chi$ (hardening/softening properties), with ζ_∞ = the initial material threshold; and $U_\infty(\chi)$ = the hardening energy (or frozen energy) in the material at complete hydration. The linear chemo-plastic hardening thus assumes a linear increase of the frozen energy $U(\chi, m)$ with respect to hydration mass m. It is noteworthy, that the term "frozen" refers to the dissipation associated with plastic evolutions. In fact, the energy associated with irreversible skeleton evolutions, which is dissipated into heat during time interval dt [see (8)], is not the energy $\varphi^p dt = \boldsymbol{\sigma}:d\boldsymbol{\varepsilon}^p$, but the energy $\varphi_1 dt = \varphi^p dt - dU$; energy $dU = m(dU_\infty - \zeta_\infty d\chi)$ thus appears as an infinitesimal energy that is neither converted into heat during the time interval dt of plastic loading, nor immediately recovered as useful (elastic) work during load reversal, but "frozen" due to chemo-plastic hardening.

From a physical standpoint, the origin of this frozen energy can be associated with a micro-elasticity of the matter constituting concrete. More precisely, at the level of the composite structure (cement paste, aggregates), the shrinkage induced by capillary action—as well as by thermal gradients—during

concrete hardening cannot be considered as homogeneous and results in a complex state of microstress, accompanied by irreversible skeleton deformation as random creation of microvoids and microcracks, that was intensively studied in the past (e.g., Wittmann et al. 1984; Roelfstra et al. 1985). Owing to the microscopic geometry of the matrix, these permanent microskeleton deformations are not homogeneous and not kinematically compatible alone, without an elastic deformation contributing to the total one, even after a complete unloading. This implies that a certain amount of energy, associated with this microelasticity, which has not been converted into heat form during loading, is not recovered nor transformed into work during unloading. Here lies the origin of the frozen energy, which is altered as a consequence of capillary action induced by hydration (chemical hardening) as well as of stress release of zones elastically deformed (plastic hardening/softening) when the skeleton undergoes permanent deformation. In the modeling at the level of the reactive porous media, the first is taken into account by hydration mass m, and the second by hardening variable χ, which both characterize the hardening state, i.e., the frozen energy $U(\chi, m)$ of the hydrating matter.

For the evolution of the plastic variables, standard expressions can be applied for both the flow rule and the hardening rule

$$d\boldsymbol{\varepsilon}^p = d\lambda \frac{\partial g(\boldsymbol{\sigma}, \zeta)}{\partial \boldsymbol{\sigma}} \qquad (22)$$

$$d\chi = d\lambda \frac{\partial h(\boldsymbol{\sigma}, \zeta)}{\partial \zeta} \qquad (23)$$

where $d\lambda$ = plastic multiplier; and $g(\boldsymbol{\sigma}, \zeta)$ and $h(\boldsymbol{\sigma}, \zeta)$ = plastic and hardening potentials. Eqs. (22) and (23) are the same as in the standard plastic model. In return, the plastic multiplier and the hardening modulus read in a modified form. In fact, the consistency condition is written in the form

$$df = 0 \Leftrightarrow \frac{\partial f}{\partial \zeta} \frac{\partial \zeta(\chi, m)}{\partial \chi} d\chi = -d_x f = -d\lambda H \qquad (24)$$

where $d_x f$ = subdifferential of loading function f at constant values of hardening variable χ; and H = hardening modulus. Then, using hardening rule (23) and expression (21) in the previous equation, leads to the following modified expressions of plastic multiplier $d\lambda$ and hardening modulus H:

$$d\lambda = \frac{d_x f}{H} = \frac{1}{H}\left[\frac{\partial f}{\partial \boldsymbol{\sigma}}:d\boldsymbol{\sigma} + \frac{\partial f}{\partial \zeta}\left(\zeta_\infty - \frac{\partial U_\infty}{\partial \chi}\right) dm\right] \qquad (25)$$

$$H = -\frac{\partial f}{\partial \zeta}\frac{\partial \zeta}{\partial \chi}\frac{d\chi}{d\lambda} = mH_\infty; \quad H_\infty = \frac{\partial f}{\partial \zeta}\left[\frac{\partial^2 U_\infty(\chi)}{\partial \chi^2}\right]\frac{\partial h}{\partial \zeta} \qquad (26)$$

where H_∞ = the hardening modulus at complete hydration. The first term in the brackets on the right hand side of (25) corresponds to the standard format of the plastic multiplier in the plastic hardening/softening model, while the second term is due to the chemical hardening. Eq. (26) for hardening modulus H is coherent with the standard definition of the sign of the hardening modulus, which is positive for hardening strictly speaking (with $d_x f > 0$) and negative in the case of softening (with $d_x f < 0$), and ensures the non-negativity of plastic multiplier $d\lambda$ (≥ 0), (Coussy and Ulm 1995). Furthermore, the modeling of chemo-plastic couplings, as presented here previously, can be used without any further restrictions concerning loading surface $f(\boldsymbol{\sigma}, \zeta)$, plastic potential $g(\boldsymbol{\sigma}, \zeta)$, and hardening potential $h(\boldsymbol{\sigma}, \zeta)$ than those imposed for the standard plastic model, i.e., convexity and non-negativeness of the intrinsic dissipation associated with irreversible skeleton evolutions. The latter reads

$$\varphi_1 dt = d\lambda \left(\boldsymbol{\sigma}:\frac{\partial g}{\partial \boldsymbol{\sigma}} + \zeta \frac{\partial h}{\partial \zeta}\right) \geq 0 \quad \text{if } f = df = 0 \qquad (27)$$

which, owing to the non-negativity of plastic multiplier $d\lambda$, defines the thermodynamic admissible directions $\partial g/\partial\sigma$ and $\partial h/\partial\zeta$ taken by the plastic increments $d\varepsilon^p$ and $d\chi$, according to the flow and hardening rules, (22) and (23). In the particular case of a linear chemo-plastic coupling (21), the extension of any standard plastic model to the case of maturing concrete is then straightforward with minor modifications concerning the plastic multiplier $d\lambda$ and hardening modulus H according to relations (25) and (26). In addition, even in the absence of plastic evolutions ($d\lambda = 0$), with hardening variable χ remaining constant, the elasticity domain may evolve due to the dependence of the hardening force ζ on hydration mass m and thus on its evolution $dm = \dot{m}dt$, in time interval dt. This evolution needs to be determined from an evolution law, the macroscopic hydration kinetics.

Macroscopic Hydration Kinetics

As mentioned previously, the diffusion of water through the layers of hydrates can be considered as the dominant mechanism governing the kinetics of hydration. According to (1), mass rate $\dot{m}$ can be viewed as a measure of this diffusion rate. It is controlled by the thermodynamic imbalance (affinity A_m) between free water and water combined in the solid phase, and amplified by thermal activation when the free water combines with unhydrated cement to form new hydrates (see Fig. 1). An evolution law of the Arrhenius type may be adopted, reading

$$A_m = \eta \frac{dm}{dt} \exp\left(\frac{E_a}{RT}\right) \qquad (28)$$

where E_a = hydration activation energy; and R = the universal constant for ideal gas. From a pure phenomenological standpoint, evolution laws based upon the Arrhenius concept are widely used since they have shown good agreement with experimental data (see, for instance, Acker 1988; Emborg 1989; Torrenti 1992). From the standpoint of standard thermodynamics, kinetic law (28) refers to expression (5) of chemical dissipation $\varphi_{\to sk}$: according to (5) the evolution law needs to be specified by a relation linking the force A_m to the rate of water consumption dm/dt. From a physico-chemical point of view, the complementary evolution law (28) accounts for two distinct phenomena. First, that rate $\dot{m}$ is controlled by the rate at which the free water diffuses through the layers of hydrates already formed. This diffusion rate depends at a microscopic scale on the gradient between the free water and the water combined in the hydrates. At the macroscopic modeling level, this gradient is expressed by affinity A_m, the driving force of the microdiffusion process, from where we get the relation $A_m = \eta\dot{m}$. Second, that the combination of water with cement is activation controlled, which the Arrhenius term $\exp(E_a/RT)$ takes into account. The first is at the basis of the chemical dissipation amplified by the latter thermal activation. Finally, viscosity η accounts for this microdiffusion. It may not be constant, because the free water has to bypass the increasing layers of hydrates in order to meet unhydrated cement and form new hydrates [i.e., $\eta = \eta(m)$].

Now, consider incremental state (13), which we recall

$$dA_m = -\mathbf{B}:(d\varepsilon - d\varepsilon^p) - L_m \frac{dT}{T_o} + \left(\zeta_\infty - \frac{\partial^2 U_\infty}{\partial\chi^2}\right) d\chi - \frac{\partial^2\psi}{\partial m^2} dm \qquad (29)$$

The previous equation shows the counterparts of the chemomechanical, chemo-thermal, and chemo-plastic couplings due to Maxwell symmetries. It indicates a dependence of affinity A_m on strain ε and ε^p, temperature T, and hardening variable χ, which can a priori induce a thermodynamic imbalance between the free water and the water combined in the solid

phase, and modify the hydration process. More precisely, the first term of (29) leads on account of (14) to a stress induced imbalance, and the second on account of (16) or (17) to a temperature-induced imbalance under nonisothermal conditions. The first two couplings and their experimental verification are discussed in some details in Ulm and Coussy (1995), and except for some special applications in concrete technology, in which high pressure and temperature are used to modify the hydration products, these couplings can be considered as weak. The third term in (29) presents on account of (23) the imbalance induced by plastic hardening/softening phenomena, and accounts in the modeling for a (possible) effect of cracking on the hydration amplitude. However, little has been reported on this subject. In a first approximation, we may consider this coupling as weak. Then, applying this partial decoupling hypothesis to (29) and integrating, the affinity A_m depends only on hydration mass m, and kinetic law (28) becomes

$$A_m \cong A_{mo} - a(m) = \eta \frac{dm}{dt} \exp\left(\frac{E_a}{RT}\right) \quad \text{with } a(m) = \int \frac{\partial^2\psi}{\partial m^2} dm \qquad (30)$$

where A_{mo} = the initial affinity that expresses the initial difference in chemical potentials between the free water and the solid phase, which starts the reaction. In turn, $a(m)$ = the balanced part of this potential difference, and depends due to the partial decoupling hypothesis only on the water mass m combined in the solid phase. Consequently, at thermodynamic equilibrium, for which the diffusion rate $\dot{m}$ is zero, we have

$$\frac{dm}{dt} = 0 \Leftrightarrow A_{mo} = a(m_\infty) \qquad (31)$$

where m_∞ = asymptotic value of the water mass combined in the solid phase. According to chemical equilibrium (31), m_∞ depends only on initial affinity A_{mo}, [i.e., $m_\infty = m_\infty(A_{mo})$], which, in turn, depends on characteristics relative to the concrete mix design, as for instance the water/cement ratio w/c

$$A_{mo} = A_{mo}(w/c, \ldots) \qquad (32)$$

Furthermore, (31) allows us to define the hydration degree in the following way:

$$\xi(t) = m(t)/m_\infty \qquad (33)$$

which varies between 0 and 1. This definition is similar to standard definitions of the hydration degree in cement chemistry (e.g., Powers and Brownyard 1948), as the weight fraction at time t of reacted cement or of nonevaporable water, which can be accessed experimentally by X-ray diffraction, nonevaporable water methods, etc. (for a comparison of different methods, see for instance Parrott et al. 1990). Here, in the modeling, expression (33) of hydration degree $\xi(t)$ combines the partial decoupling hypothesis (30) with the chemical equilibrium condition, expressed by (31) at the macroscopic level of material modeling. It constitutes an intrinsic definition for the hydration degree of a given concrete mix, provided that the thermodynamic imbalance induced by variations in strain, temperature, and irreversible skeleton evolution can be neglected with respect to the initial affinity A_{mo}. Furthermore, definition (33) together with (30) and (31) allows us to rewrite the macroscopic kinetic law in the form

$$\tilde{A}(\xi) = \frac{d\xi}{dt} \exp\left(\frac{E_a}{RT}\right) \qquad (34)$$

where $\tilde{A}(\xi)$ can be considered as a normalized affinity [$\tilde{A} \sim A_m(\xi)/\eta(\xi)$]. It accounts for the chemical nonequilibrium, $A_m = A_m(\xi)$, as well as for the nonlinear diffusion process, ex-

pressed by $\eta = \eta(\xi)$, of free water through the increasing layers of hydrates already formed. Due to the partial decoupling hypothesis, the normalized affinity $\tilde{A}$ depends only on hydration degree ξ. This function $\tilde{A} = \tilde{A}(\xi)$ characterizes the macroscopic hydration kinetics, and allows, for a given temperature history $T(t)$, the determination of hydration degree $\xi(t)$, and thus of the solidification state of the material.

Finally, it is worthwhile to derive the relation that links this kinetic approach with other common aging models, where an equivalent age (or "maturity") is used defined by

$$\mu = \int_0^t \exp\left[\frac{E_a}{R}\left(\frac{1}{T_o} - \frac{1}{T(\tau)}\right)\right] d\tau \tag{35}$$

where T_o = reference temperature, for which maturity μ coincides with time. Using (35) in (34), the hydration kinetics is described by an ordinary differential equation

$$\frac{d\xi}{d\mu} = c\tilde{A}(\xi) \tag{36}$$

where $c = \exp(-E_a/RT_o)$. The previous equation reveals a relation of the form

$$\xi = \xi(\mu) \tag{37}$$

that links the hydration degree ξ to the maturity μ. Relation (36) can so be used to replace in constitutive equations based upon the maturity concept, maturity μ by hydration degree ξ, the evolution of which is governed by kinetic law (34).

MACROSCOPIC INVESTIGATION OF HYDRATION KINETICS

As just seen, function $\tilde{A}(\xi)$ plays a major role in the modeling of the hydration reaction, and consequently for the determination of its effects on strain, strength growth, and heat generation. According to (34), its experimental determination requires for a given temperature history $T(t)$ the measurement of the evolution of hydration degree $\xi(t)$, according to definition (33), as weight-fraction of reacted cement or nonevaporable water. Alternatively, the hydration degree can be accessed experimentally by exploring consequently the thermo-chemo-mechanical couplings, i.e., the Maxwell symmetries. The experimental data on temperature and strength evolution of high performance and ordinary concretes used hereafter were presented by Laplante (1993). The high performance concrete (HPC) is characterized by a water:cement ratio w/c = 0.3 and a silica fume:cement ratio s/c = 0.1, and the ordinary concrete (OC) by w/c = 0.5. (For preparation, curing conditions, etc., see Laplante 1993.)

Adiabatic Calorimetric Experiment

The determination of the hydration degree from calorimetric experiments is current standard (RILEM 1994). In terms of the theory presented here, this approach consists in exploring the linear thermo-chemical coupling in heat (17), which on account of the variable change $m \to \xi$ becomes

$$C_\varepsilon \frac{dT}{dt} = Q^0 + L \frac{d\xi}{dt} \tag{38}$$

where $L = L_m m_\infty$ = latent heat per unit of hydration degree $d\xi$; while Q^0 = heat rate provided from the exterior. In an adiabatic experiment, in which this external heat rate is zero, $Q^0 = 0$, the exothermic nature of the hydration reaction ($L > 0$) leads to temperature elevation, as shown in Fig. 3 for the high performance concrete. Noting $T^{ad}(t)$ the temperature of the concrete as a function of time t in the adiabatic experiment, the combination of definition (33) with entropy balance (38) yields
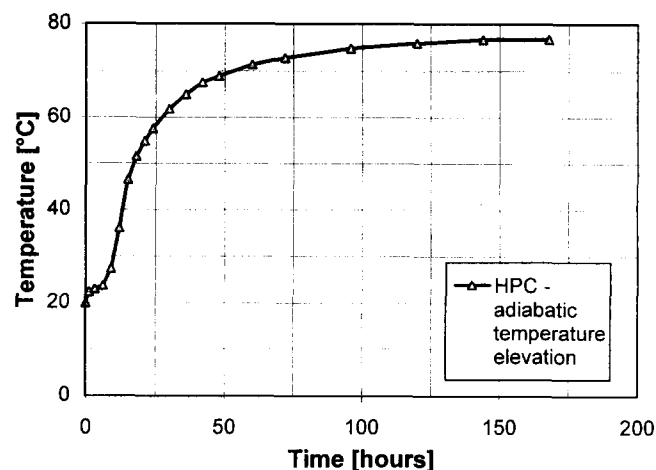
FIG. 3. Temperature Elevation in °C of High Performance Concrete in Adiabatic Experiment, with $T^{ad}(\infty) - T_o = 60$ K

$$\xi(t) = \frac{T^{ad}(t) - T_o}{T^{ad}(\infty) - T_o} \tag{39}$$

where T_o and $T^{ad}(\infty)$ are the initial and the final temperature in the considered experiment, respectively. Furthermore, equations (39) and kinetic law (34) imply the following identification of kinetic function $\tilde{A}(\xi)$:

$$\tilde{A}(\xi) = \frac{1}{T^{ad}(\infty) - T_o} \frac{dT}{dt}(t)\exp\left[\frac{E_a}{RT^{ad}(t)}\right] \tag{40}$$

With $T^{ad}(t)$ being a measurable function of time, (39) and (40) lead to determine function $\tilde{A}(\xi)$ in a parameter form of time t of the adiabatic experiment. This is shown in Fig. 4 for the temperature evolution given in Fig. 3. The activation energy E_a used in this determination corresponds to $E_a/R = 4000$ K, determined previously for this type of concrete mix (Laplante 1993).

The previous identification of kinetic function $\tilde{A}(\xi)$ can be applied to other calorimetric experiments, for instance carried
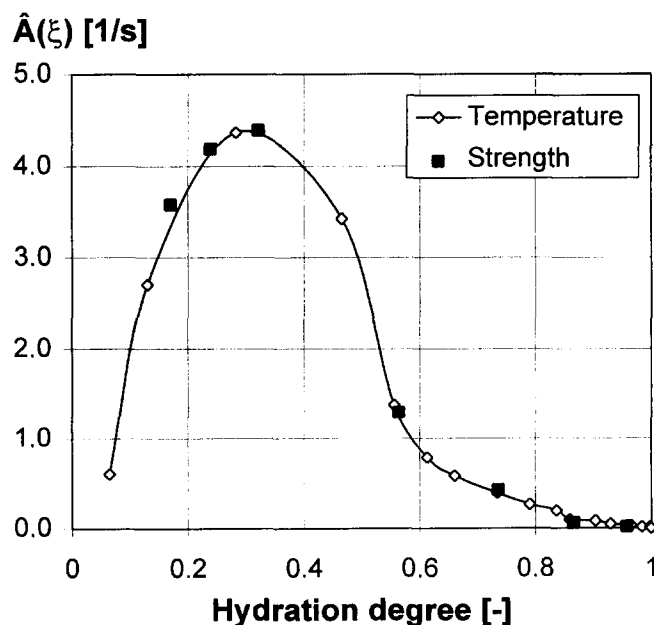

FIG. 4. The Normalized Affinity $\tilde{A}$ of High Performance Concrete as Function of Hydration Degree, Determined from Adiabatic Temperature Elevation [i.e., Eq. (40) versus (39), Curve Named "Temperature"] and from Isothermal Strength Evolution [i.e., Eq. (43) versus (42), Curve Named "Strength"] (Experimental Values from Laplante 1993)

out under isothermal conditions ($\dot{T} = 0$) on the same concrete, and can be used to confirm the linearity of the thermo-chemical coupling taken into account in the modeling, as well as the validity of the partial decoupling hypothesis with respect to temperature variation. However, they cannot confirm the intrinsic character of the found function $\tilde{A}(\xi)$, and thus the validity of the approach. Another experiment, independent of the calorimetric one, is required, which gives experimental access to the evolution of hydration degree $\xi(t)$.

Isothermal Strength Evolution

To this end, we can explore the chemo-plastic coupling, as presented before, which accounts for the strength growth as chemical hardening. In particular, the isothermal evolution of the material strength, as illustrated in Fig. 5 for the high performance concrete and the ordinary concrete, lends itself readily for the experimental determination of kinetic function $\tilde{A}(\xi)$. More precisely, from an experimental point of view, it has been shown that the isothermal evolution of the compressive strength $f_c(t)$ is thermal-activated (Regourd and Gauthier 1980), and that its increase df_c is proportional to the increase $d\xi = dm/m_\infty$ in hydration products (Mindess et al. 1978; Byfors 1980; Laube 1990; Torrenti 1992), thus

$$\frac{df_c}{dt} = c \frac{d\xi}{dt} \tag{41}$$

where c is a constant. In the theory, this is taken into account by the linear dependence of hardening force ζ on hydration mass m [i.e., (21)], the evolution of which is given by kinetic law (34). Exploring this linear chemo-plastic coupling for the material strength $\zeta = f_c = mf_c(\infty)$, (33) and (41) lead to

$$\xi(t) = \frac{\zeta(t) - \zeta_o}{\zeta(\infty) - \zeta_o} \tag{42}$$

where $\zeta(\infty)$ is the material strength at complete hydration, and ζ_o (≤ 0) a reference value for $\xi = 0$, which accounts for a solidification threshold ξ_o concerning the material strength, as illustrated in Fig. 6 (e.g., Laube 1990). Eqs. (34) and (42) then yield

$$\tilde{A}(\xi) = \frac{1}{\zeta(\infty) - \zeta_o} \frac{d\zeta}{dt} (t) \exp\left(\frac{E_a}{RT_o}\right) \tag{43}$$

where T_o = temperature in the isothermal material strength experiments. Eqs. (42) and (43) are of the same format as relations (39) and (40), and constitute a second experimental access to kinetic function $\tilde{A}(\xi)$, independent of the former
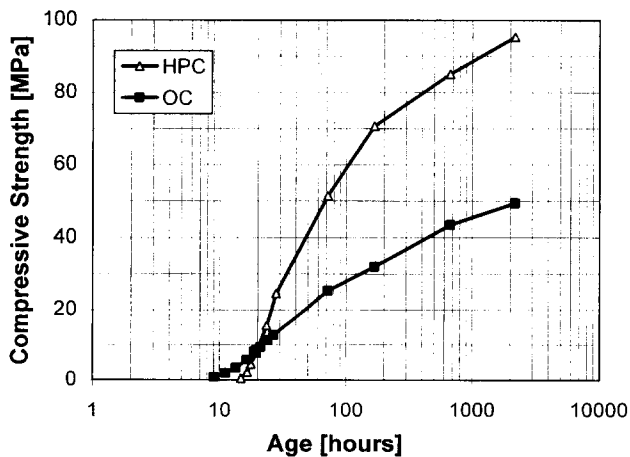

FIG. 5. Evolution of Compressive Strength as Function of Time, for High Performance Concrete [HPC, $f_c(\infty)$ = 100 MPa] and Ordinary Concrete [OC, $f_c(\infty)$ = 50 MPa] (Experimental Values from Laplante 1993)
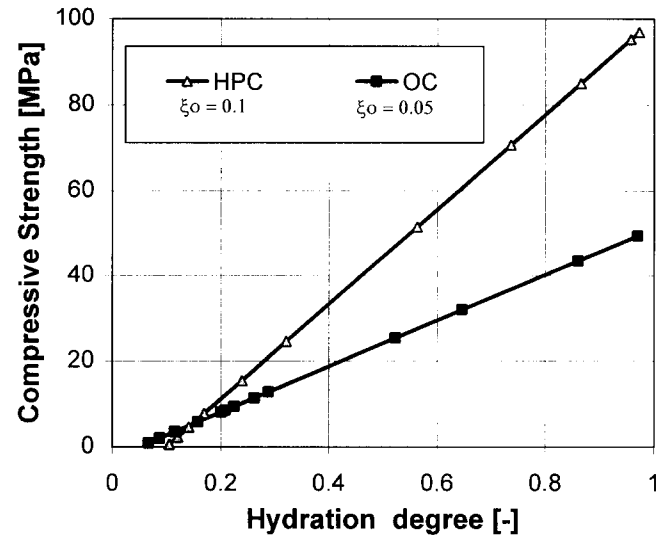

FIG. 6. Linear Chemo-Plastic Coupling: Evolution of Compressive Strength as Function of Hydration Degree, with ξ_o the Solidification Threshold for High Performance Concrete (HPC, ξ_o = 0.1) and Ordinary Concrete (OC, ξ_o = 0.05)

calorimetric one. This is shown in Fig. 4 (curve named "Strength"), determined from the isothermal compressive strength evolution of the high performance concrete. The values for $\tilde{A}(\xi)$ determined for this concrete from two independent experiments, a calorimetric and a mechanical one, coincide and confirm the intrinsic nature of kinetic function $\tilde{A}(\xi)$. This agreement has to be seen in relation with the thermal activation of the hydration reaction, which implies for the hydration rate to be much greater in the adiabatic calorimetric test than in the isothermal strength tests. This confirms a posteriori the nonsignificant influence of temperature variation on affinity A_m, and thus the partial decoupling hypothesis with respect to temperature variation.

Isothermal Autogeneous Shrinkage

As just seen, the hydration kinetics can be determined directly at the macroscopic level of material description by exploring the Maxwell symmetries of the modeling. This requires the knowledge of the order of coupling, as for instance the linear thermo-chemical coupling or the linear chemo-plastic one, used here before. The order of the chemo-mechanical coupling that results in autogeneous shrinkage is illustrated in Fig. 7 and shows the autogeneous shrinkage as a function of hydration degree ξ (determined from the compressive strength evolution) for the high performance concrete and the ordinary one. The slope of this curve presents with opposite sign the chemical dilatation coefficient $\beta = \beta(\xi)$, as introduced in state (14). We note that $\beta \approx$ const for low hydration degrees, and independent of the type of concrete. For hydration degrees $\xi > 0.6$, this linear chemo-mechanical coupling is lost, probably due to the strong nonlinearity of capillary actions, in particular in high performance concretes with low water-cement ratios (Baroghel-Bouny 1994).

DRUCKER-PRAGER CRITERION WITH ISOTROPIC CHEMICAL HARDENING

Finally, to illustrate the previous developments for concrete as a thermo-chemo-plastic material, we show hereafter the application of chemo-plastic hardening with a simple isotropic yield criterion, the Drucker-Prager one, with isotropic hardening. The loading function reads

$$\sigma \in C_E \Leftrightarrow f = \tau + f[\sigma - k(m, \chi)] \leq 0 \tag{44}$$
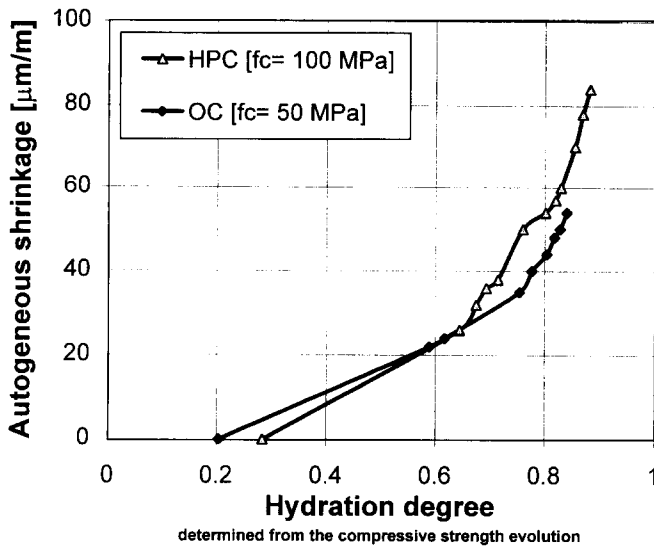
FIG. 7. Nonlinear Chemo-Mechanical Coupling: Evolution of Autogenous Shrinkage as Function of Hydration Degree, for High Performance Concrete (HPC) and Ordinary Concrete (OC) (Experimental Values from Laplante 1993)

where $\sigma = (1/3)\text{tr } \boldsymbol{\sigma}$ and $\tau = \sqrt{(1/2)\mathbf{s:s}}$ = stress invariants (with $\mathbf{s} = \boldsymbol{\sigma} - \sigma 1$); $f (\geq 0)$ = the coefficient of internal friction; and $k(m, \chi) \geq 0$ = the cohesive pressure that describes the transformation of the yield surface due to isotropic chemo-plastic hardening/softening. Using (21) together with (33) and (42), the latter can be expressed as a function of hydration degree ξ as follows:

$$k(m, \chi) = k_o - \zeta(\xi, \chi); \quad \zeta(\xi, \chi) = -\xi(k_\infty - k_o) - \xi \frac{\partial U_\infty(\chi)}{\partial \chi} \quad (45)$$

where $k_\infty (=\zeta_\infty)$ = the cohesive pressure at complete hydration; and $k_o (=\zeta_o \leq 0)$ = the reference cohesive pressure. In expression (45) of hardening force $\zeta(\xi, \chi) \leq k_o$, the term $-\xi(k_\infty - k_o)$ accounts for pure chemical hardening (i.e., the strength growth) while the term $-\xi \partial U_\infty(\chi)/\partial \chi$ is associated with plastic hardening and softening.

For the plastic flow rule, consider a nonassociated plastic potential g reading

$$g = \tau + \delta[\sigma - k_o + \zeta(\xi, \chi)] \quad (46)$$

where δ = dilatancy factor, which is assumed constant. Then, using (22) and splitting the tensor of plastic strain increment $d\boldsymbol{\varepsilon}^p$ in its deviator and volume part, leads to:

$$d\boldsymbol{\varepsilon}^p = d\mathbf{e}^p + (1/3)d\varepsilon^p 1; \quad d\mathbf{e}^p = d\lambda(\mathbf{s}/2\tau); \quad d\varepsilon^p = \text{tr}(d\boldsymbol{\varepsilon}^p) = d\lambda\delta \quad (47)$$

Furthermore, using as hardening potential h the plastic potential g as given by (46) in (23), the hardening rule reads here

$$d\chi = d\lambda \frac{\partial g}{\partial \zeta} = d\lambda\delta \quad (48)$$

The latter together with flow rule (47) leads to identify the plastic volume variation as the hardening/softening variable χ

$$d\chi = d\varepsilon^p = d\lambda\delta \Rightarrow \chi = \varepsilon^p = \text{tr } \mathbf{e}^p \quad (49)$$

Consistency condition (24) then reads here

$$\frac{\partial f}{\partial \zeta} \frac{\partial \zeta(\xi, \varepsilon^p)}{\partial \varepsilon^p} d\varepsilon^p = -d_{\varepsilon^p}f = -d\lambda H \quad (50)$$

which, on account of relations (45) and (49), yields expression (26) of hardening modulus H in the form

$$H = \xi H_\infty; \quad H_\infty = -f \frac{\partial \zeta(\xi, \varepsilon^p)}{\partial \varepsilon^p} \frac{d\varepsilon^p}{d\lambda} = f \frac{\partial^2 U_\infty(\varepsilon^p)}{\partial \varepsilon^{p^2}} \delta \quad (51)$$

where $U_\infty(\varepsilon^p)$ = plastic hardening energy of the material at complete hydration; and H_∞ = corresponding hardening modulus. It is interesting to note that for $\xi \to 0$ the material behaves as an ideal plastic material, and achieves its hardening/softening capacity with the hydration advancing. This linear dependence of the plastic material properties on hydration degree ξ, needs however still to be confirmed from experimental data of hardening and softening of early age concrete [for instance, from fracture energy G_f that is proportional to frozen energy $U(\chi, \xi)$, as a function of hydration degree ξ].

Furthermore, the plastic multiplier $d\lambda$ is obtained according to (25) from (50) in the form

$$d\lambda = \frac{d_{\varepsilon^p}f}{\xi H_\infty} = \frac{d\tau + fd\sigma}{\xi H_\infty} - \frac{f}{H_\infty}\left(k_\infty - k_o + \frac{\partial U_\infty}{\partial \varepsilon^p}\right)\frac{d\xi}{\xi} \quad (52)$$

where $d\tau = \mathbf{s}:d\mathbf{s}/2\tau$ and $d\sigma = (1/3)\text{tr}(d\boldsymbol{\sigma})$. In addition, the thermodynamic restrictions imposed by (27) together with (47) and (48), imply

$$\varphi_1 dt = d\lambda[\tau + \delta(\sigma + \zeta)] \geq 0 \quad \text{if } f = df = 0 \quad (53)$$

where we recall that $\varphi_1 dt$ is the heat produced by dissipation due to plastic evolutions in time interval dt. Then replacing in the previous expression τ by that given for $f = 0$ from yield criterion (44), yields

$$\varphi_1 dt = d\lambda[(\sigma + \zeta)(f + \delta) - fk_o] \geq 0 \quad (54)$$

Since $d\lambda \geq 0$ and $f \geq 0$, the previous inequality is satisfied for $k_o \leq 0$ and $0 \leq \delta \leq f$. The first condition implies $k_\infty \geq 0$, since, according to (42), $k_o = -k_\infty \xi_o/(1 - \xi_o)$; where ξ_o = solidification threshold. The second implies the non-negativity of the plastic dilatation (i.e., $d\varepsilon^p \geq 0$). Note that these restrictions, the non-negativity of cohesive pressure k_∞ and of the plastic dilatation, are intrinsic to plastic models of the Drucker-Prager type irrespective of chemo-plastic couplings and hardening/softening phenomena (whether isotropic or kinematic). This illustrates that the proposed extension of the classical elastoplastic theory to the case of chemo-plastic couplings can be used together with any loading function, plastic potentials and hardening potential without any further restrictions than those imposed for the standard plastic model.

Finally, the Drucker-Prager plastic model with chemo-plastic hardening as presented here previously is to be considered as a first approximation, particularly due to the assumed isotropy of chemical and plastic hardening, which cannot account for a dependence of the friction angle f on the hydration degree, or on the stresses. In fact, the preceding example only sought to show how to account for the evolution of the plastic properties (crack threshold and hardening/softening properties) with the hydration advancing in a standard model of the Drucker-Prager type. Furthermore, the choice of the plastic model is not restrictive. The presented modeling of chemo-plastic couplings can be equally applied—with minor modifications—to other crack models for concrete at early ages, as for instance to damage models (Bournazel 1992), smeared crack models (de Borst and van den Boogaard 1994), plastic degrading (or plastic damage) models (Coussy and Ulm 1995), or discrete crack models (Ulm et al. 1995).

CONCLUSIONS

This paper explores macroscopic thermo-chemo-mechanical couplings in early age concrete, on account of irreversible skeleton evolution (i.e., cracking) and chemo-plastic couplings (i.e., strength growth). The term "macroscopic" means here that the modeling employs only quantities proper to the mac-

roscopic scale (typically, the laboratory test specimen size) adopted for the continuous description of the evolutions of the closed reactive porous media. The main points to be noted are

1. The proposed model for concrete at early ages accounts explicitly for the hydration reaction at the macroscopic level of material description by means of a macroscopic variable, the solidification mass m. The effects of the chemical reaction on temperature evolution, deformation and cracking (the "coupling") result naturally from the Maxwell symmetries, a consequence of the chosen thermodynamic approach. They lead to account for autogenous shrinkage; hydration heat; and strength growth due to chemo-mechanical, thermo-chemical and chemo-plastic couplings, with a minimum of material parameters of clear physical significance. These Maxwell symmetries provide a macroscopic access (both theoretically and experimentally) to the hydration degree ξ provided that the order of coupling is known, as for instance the linear thermo-chemical coupling or the linear chemo-plastic one.

2. The model considers concrete cracking at early ages with plastic variables, modeling the irreversible skeleton deformation within the hypothesis of continuity. The proposed extension of the classical elastoplastic theory to the case of chemo-plastic couplings to account for strength growth, as well as for the evolution of the plastic/hardening properties of maturing concrete, can be used together with any loading function, plastic potential, and hardening potential, without any further restriction than those imposed for the standard plastic model. This is illustrated for the Drucker-Prager criterion with isotropic chemo-plastic hardening.

3. The diffusion of free water through the layers of hydrates to unhydrated cement is considered as the dominant mechanism governing the hydration kinetics, and thus the kinetics of the measurable macroscopic phenomena. In other words, the kinetics can be considered as a linkage between these different scales. To integrate this micro-mechanism in the macroscopic modeling, a kinetic law is proposed that links the driving force (i.e., the potential difference between the free water and the water combined in the solid phase) to the rate of solidification mass. Assuming the thermodynamic imbalance induced by stress, temperature and plastic evolutions negligible for the hydration reaction, the "normalized affinity" is identified as an intrinsic kinetic function, which characterizes the macroscopic hydration kinetics of concretes. It depends only on hydration degree ξ. Due to Maxwell symmetries, this function can be determined from standard material tests, such as calorimetric tests or material strength evolution tests.

4. Creep effects were not yet considered in the modeling. In fact, assuming that the thermodynamic imbalance of the hydration reaction does not depend on the stress applied, possible creep effects related to the hydration reaction were eliminated in the modeling. This seems consistent with physical evidence, since it implies that the hydration is not at the physical origin of apparent creep effects under external load application. However, the matrix behavior shows some non-negligible hereditary aspects, not taken into account in the modeling. More precisely, due to the capillary traction related to the water consumption in the hydration reaction, the skeleton suffers an increasing internal compression, which gives rise to creep effects intrinsic to the matrix even in the absence of external load application. Then, a part of the shrinkage deformation measured under isothermal and load free

conditions are due to these creep effects. In this case, the autogenous shrinkage needs to be seen as the superposition of two distinct physical processes: the microdiffusion process associated with the hydration reaction and the intrinsic creeping of the matrix. The latter, however, may as well be due to a microdiffusion process at the scale of the maturing matrix (e.g., Bažant 1972, Bažant and Moschovidis 1973)—still to be explored within the macroscopic modeling of thermo-chemo-mechanical couplings of concrete at early ages.

APPENDIX I.   REFERENCES

Acker, P. (1988). "Comportement mécanique du béton: apports de l'approche physico-chimique (Mechanical behavior of concrete: a physico-chemical approach)." Res. Rep. LPC, 152, Laboratoires des Ponts et Chaussées (LPC), Paris, France (in French).

Baroghel-Bouny, V. (1994). "Charactérisation des pâtes de ciment et des bétons: méthodes, analyse, interprétations (Characterization of cement pastes and concretes: methods, analysis, interpretations)," PhD thesis, Ecole Nationale des Ponts et Chaussées, Paris, France.

Bažant, Z. P. (1972). "Thermodynamics of interacting continua with surface and creep analysis of concrete structures." Nuclear Engrg. and Des., 20, 477–505.

Bažant, Z. P., and Moschovidis, Z. (1973). "Surface diffusion theory for the drying creep effect in portland cement paste and concrete." J. Am. Ceramic Soc., 56, 235–241.

Bažant, Z. P. (1977). "Viscoelasticity of porous solidifying material—concrete." J. Engrg. Mech. Div., ASCE, 103(6), 1049–1067.

Bažant, Z. P., and Prasannan, S. (1989a). "Solidification theory for concrete creep. I: formulation." J. Engrg. Mech., ASCE, 115(8), 1691–1703.

Bažant, Z. P., and Prasannan, S. (1989b). "Solidification theory for concrete creep. II: verification and application." J. Engrg. Mech., ASCE, 115(8), 1704–1725.

Bažant, Z. P. (1995). "Creep and damage in concrete." Material science of concrete IV, J. Skalney and S. Mindess, eds., Am. Ceramic Soc., Westerville, Ohio, 335–389.

Bournazel, J. P. (1992). "Contribution à l'étude du caractère thermomécanique de la maturation des bétons (Analysis of the thermomechanical character of maturing concrete)," PhD thesis, Université Paris 6, Paris, France (in French).

Buil, M. (1979). "Contribution à l'étude du retrait de la pâte de ciment durcissante (Analysis of shrinkage of hardening cement paste)," PhD thesis, Ecole Nationale des Ponts et Chaussées, Paris, France (in French).

Byfors, J. (1980). "Plain concrete at early ages." Res. Rep. F3:80, Swedish Cement and Concrete Res. Inst., Stockholm, Sweden.

Carol, I., and Bažant, Z. P. (1993). "Viscoelasticity with aging caused by solidification of nonaging constituent." J. Engrg. Mech., ASCE, 119(11), 2252–2269.

Coussy, O. (1995). Mechanics of porous continua. J. Wiley & Sons, Inc., Chichester, England.

Coussy, O., and Ulm, F. J. (1995). "Creep and plasticity due to chemomechanical couplings." Computational plasticity. fundamentals and applications, (Proc., 4th Int. Conf. Complas IV). Pineridge Press, Swansea, Wales, 925–944.

de Borst, R., and van den Boogaard, A. H. (1994). "Finite-element modeling of deformation and cracking in early-age concrete." J. Engrg. Mech., ASCE, 120(12), 2519–2534.

Emborg, M. (1989). "Thermal stresses in concrete structures at early ages," PhD thesis, Lulea University of Technology, Lulea, Sweden.

Hua, C. (1992). "Analyses et modélisation du retrait d'autodessiccation de la pâte de ciment durcissante (Analysis and modeling of autodessiccation shrinkage of hardening cement paste)," PhD thesis, Ecole National des Ponts et Chaussées, Paris, France (in French).

Huckfeldt, J. (1993). "Thermomechanik hydratisierenden Betons—theorie, numerik und anwendung (Thermo-mechanics of hydrating concrete—theory, numerics and application)," PhD thesis, TU Braunschweig, Braunschweig, Germany (in German).

Laplante, P. (1993). "Propriétés mécaniques des bétons durcissants: an-

alyse comparée des bétons classiques et à très hautes performances (Mechanical properties of hardening concrete: a comparative analysis of ordinary and high performance concretes)," PhD thesis, Ecole Nationale des Ponts et Chaussées, Paris, France (in French).

Laube, M. (1990). "Werkstoffmodell zur Berechnung von Temperaturspannungen in massigen Betonbauteilen im jungen alter (Constitutive model for the analysis of temperature-stresses in massive structures of concrete at early ages)," PhD thesis, TU Braunschweig, Braunschweig, Germany (in German).

Lemaitre, J., and Chaboche, J. L. (1990). *Mechanics of solid materials.* Cambridge University Press, London, England.

Mindess, S., Young, J. F., and Lawrence, F. V. (1978). "Creep and drying shrinkage of calcium silicate pastes. I: specimen preparation and mechanical properties." *Cement and Concrete Res.*, 8, 591–600.

Parrott, L. J., Geiker, M., Gutteridge, W. A., and Killoh, D. (1990). "Monitoring portland cement hydration: comparison of methods." *Cement and Concrete Res.*, 20, 919–926.

Powers, T. C., and Brownyard, T. L. (1948). "Studies of the physical properties of hardened Portland cement paste." *Bull. No. 22*, Portland Cement Association, Skokie, Ill.

Regourd, M., and Gauthier, E. (1980). "Comportement des ciments soumis au durcissement accéléré (Behavior of cement under accelerated hardening)." *Annales de l'ITBTP, No. 387*, Paris, France, 65–96 (in French).

Reunion Internationale des Laboratoires d'Essais et de Recherches sur les Materiaux et les Constructions (RILEM). (1994). "Thermal cracking in concrete at early ages." *Proc., Int. RILEM Symposium*, R. Springenschmid, ed., E & FN Spon, London, England.

Roelfstra, P. E., Sadouki, H., and Wittmann, F. H. (1985). "Le béton numérique (The numerical concrete)." *Mat. and Struct.*, Paris, France, 18(107), 327–335 (in French).

Tanabe, T., and Ishikawa, Y. (1993). "Time-dependent behaviour of concrete at early ages and its modelling." *Creep and shrinkage of concrete [Proc., 5th Int. RILEM Symp. (ConCreep 5)]*. Z. P. Bažant and I. Carol, eds., E & FN Spon, London, England, 435–452.

Torrenti, J. M. (1992). "La résistance du béton au très juene âge (Strength of concrete at very early ages)." *Bulletin de Liaison des Laboratoires des Ponts et Chaussées*, Paris, France, 179, 31–41 (in French).

Torrenti, J. M., Guenot, I., Laplante, P., Acker, P., and de Larrard, F. (1994). "Numerical simulation of temperatures and stresses in concrete at early ages." *Computational Modelling of Concrete Structures [Proc., Int. Conf. (EURO-C 1994)]*. H. Mang, N. Bicanic, and R. de Borst, eds., Pineridge Press, Swansea, Wales, 559–568.

Ulm, F.-J., and Coussy, O. (1995). "Modeling of thermochemomechanical couplings of concrete at early ages." *J. Engrg. Mech.*, ASCE, 121(7), 785–794.

Ulm, F.-J., Elouard, A., and Rossi, P. (1995). "Modelling of early age concrete cracking due to thermo-chemo-mechanical couplings." *Fracture mechanics of concrete structures [Proc., Int. Conf. (FRAMCOS-2)], Vol. II.* F. H. Wittmann, ed., Aedificatio Publisher, Freiburg, Germany, 1143–1458.

Wittmann, F. H. (1976). "On the action of capillary pressure in fresh concrete." *Cement and Concrete Res.*, 6(1), 49–56.

Wittmann, F. H. (1982). "Creep and shrinkage mechanisms." *Creep and shrinkage in concrete structures.* Z. P. Bažant and F. H. Wittmann, eds., J. Wiley & Sons, Inc., New York, N.Y., 129–161.

Wittmann, F. H., Roelfstra, P. E., and Sadouki, H. (1984). "Simulation and analysis of composite structures." *Mat. Sci. Engrg.*, 68, 239–248.

APPENDIX II.   NOTATION

The following symbols are used in this paper:

$\tilde{A}$ = normalized affinity (kinetic function);
A = second-order thermo-mechanical coupling tensor;
A_m, A_{mo} = hydration affinity, initial affinity;
$\mathbf{a}$ = second-order tensor of thermal dilatation coefficients;
$a(m)$ = chemical equilibrium function;

B = second-order chemo-mechanical coupling tensor;
$\mathbf{b}$ = second-order tensor of chemical dilatation coefficients;
C = fourth-order elastic stiffness tensor;
C_ε = volume heat capacity;
C_E = elasticity domain;
c = constant;
$d(x)$ = increment of quantity x;
$d\lambda$ = plastic multiplier;
E = Young's modulus;
E_a = activation energy;
e, e^p = strain deviator, plastic strain deviator;
f = loading function;
f = coefficient of internal friction;
f_c = compressive strength;
G = chemical potential of water combined in the solid phase;
g = plastic potential;
g^l = chemical potential of free water;
H = hardening modulus;
h = hardening potential;
K = Kelvin;
k = cohesive pressure;
$\tilde{k}$ = conductivity;
L = latent heat of hydration per unit of hydration degree;
L_m = latent heat of hydration per unit of solidification mass;
$m = m_{l \to sk}$ = solidification mass per volume unit;
m_l = variation of free water mass per volume unit;
Q^0 = rate of external heat supply;
$\mathbf{q}$ = heat flux vector;
R = universal constant for ideal gas;
r = rate of external volume heat sources;
S = entropy;
$\mathbf{s}$ = stress deviator tensor;
s/c = silica fume:cement ratio;
T, T_o = (absolute) temperature, reference temperature;
t = time;
U = frozen hardening energy;
w/c = water:cement ratio;
$\dot{x}$ = time derivative of quantity x;
α = linear thermal dilatation coefficient;
β = linear chemical dilatation coefficient;
δ = dilatancy factor;
$\varepsilon, \varepsilon^p$ = strain tensor, plastic strain tensor;
$\varepsilon, \varepsilon^p$ = volume strain, plastic volume strain;
ζ = hardening force;
η = viscosity;
μ = maturity;
ξ = hydration degree;
σ = stress tensor;
σ = mean stress;
τ = second stress deviator invariant;
φ = intrinsic dissipation;
φ_1 = dissipation associated with irreversible skeleton evolution;
$\varphi_{\to sk}$ = dissipation associated with the hydration process;
χ = plastic hardening/softening variable;
ψ = free energy;
$():(\,)$ = double tensor contraction;
$()\cdot(\,)$ = scalar product; and
$\mathbf{1}$ = second-order unit tensor.